Available online at www.sciencedirect.com
SCIENCE DIRECT®
Journal of Chromatography A, 1050 (2004) 35–44
JOURNAL OF CHROMATOGRAPHY A
www.elsevier.com/locate/chroma

Element-selective detection in liquid and gas chromatography by diode laser absorption spectrometry

Alexander Zybin, Joachim Koch, David J. Butcher[1], Kay Niemax*

ISAS—Institute for Analytical Sciences, Bunsen-Kirchhoff-Strasse 11, 44139 Dortmund, Germany

Available online 25 June 2004

Abstract

An element-selective detector for chromatography based on atomic absorption spectrometry with semiconductor diode lasers is described. The analytical utility of the technique is demonstrated by speciation examples of HPLC and GC employing analytical flames and plasmas to atomize.

Keywords: Element-selective detection; Detection, GC; Detection, LC; Diode laser atomic absorption spectrometry

1. Introduction

This article describes the analytical capabilities of a still widely unknown powerful element-selective detection technique for chromatography, diode laser atomic absorption spectrometry (DLAAS). In our opinion, this detector has significant general applicability for speciation once laser diodes are commercially available that emit radiation across the entire ultraviolet-visible range. At the moment, DLAAS detection can solve particular problems. Some recent examples are discussed in this short review.

The paper presents a brief description of the theoretical background of AAS with diode lasers and outlines the instrumentation, with a focus on recent developments in laser diode technology that have increased its sensitivity. Examples of analytical problems are given which require HPLC for metal speciation analysis and GC for the measurement of species containing halogen elements, hydrogen, carbon, and sulfur. The HPLC examples include the determination of toxic and carcinogenic chromium(VI) with essential chromium(III) and a potentially toxic organomanganese fuel additive, methylcyclopentadienyl manganese tricarbonyl (MMT) in the presence of essential manganese(II). The GC-DLAAS examples involve measurements of halogenated hydrocarbons. Analytical results are presented which demonstrate the suitability of DLAAS to perform complicated speciation analyses with sensitive but simple and inexpensive systems which complement the element-selective detectors employed in chromatography.

The most widely used element selective techniques for chemical speciation analysis are the atomic spectrometry methods of atomic absorption (AAS), optical emission (OES), atomic fluorescence (AFS), and atomic mass spectrometries [1–4]. The most suitable atomizers for speciation analysis employ a continuous flow of sample into the instrument to allow a direct interface between a chromatography system, such as flames or plasmas [5]. Discrete atom cells, such as electrothermal atomizers (graphite furnaces) and arcs/sparks, are generally less suitable because of the difficulty of interfacing continuous flow into these devices [6]. Early speciation analysis work employed chromatography systems coupled to flames as atomizers, primarily with hollow cathode lamps (HCLs) as excitation sources for AAS. Disadvantages of HCL-AAS include relatively poor sensitivity and a short linear dynamic range (LDR).

More recently, speciation analysis work has focused upon the use of inductively coupled plasmas (ICP) for detection, using either optical emission spectrometry (ICP-OES) [7] or mass spectrometry (ICP-MS) [8]. These techniques provide better detection limits and longer LDRs than flames. ICP-MS is particularly sensitive, with detection limits below 1 part-per-trillion for many elements. In addition, ICP-MS

* Corresponding author. Tel.: +49-231-1392-101; fax: +49-231-1392-310.
E-mail address: niemax@isas-dortmund.de (K. Niemax).
[1] Present address: Department of Chemistry and Physics, Western Carolina University, Cullowhee, NC 28723, USA.

0021-9673/$ – see front matter © 2004 Elsevier B.V. All rights reserved.
doi:10.1016/j.chroma.2004.05.078

has the additional advantage of providing isotopic information which is of crucial importance in speciation studies. However, the purchase price and cost of operation of these instruments are high.

An alternative approach to speciation analysis involves the use of lasers as excitation sources for AAS or AFS. For example, Walton et al. [9] determined organomanganese compounds by HPLC with AFS detection using a flame as the atom cell, and obtained a detection limit of 0.5 ng/mL (10 pg). This system used an expensive and unreliable excimer laser system, which limits the practicability of the technique. In addition, these laser systems are pulsed lasers, operating at relatively low frequencies (maximum 500 Hz, most less than 100 Hz) and very low duty cycles. They are also very large and cumbersome to operate.

Semiconductor diode lasers (DL) are a relatively new laser source that offer high reliability, small size, and easy operation [10,11] and consequently offer the potential for low cost, high sensitivity elemental analysis. The use of DLs for AAS typically improves the sensitivity by one to three orders of magnitude while maintaining the advantages of low cost, robustness, reliability, ease of use, and widespread use. Many HPLC methods employ high concentrations of organic solvents or salts. An important advantage of AAS compared to ICP-MS is the insensitivity of a flame to these compounds compared to a plasma, providing higher flexibility for the chromatographic conditions. In summary, DLAAS provides a sensitive, low cost alternative to complicated and expensive detection systems for speciation analysis.

2. Diode laser atomic absorption spectrometry

Usually, absorption measurements are not considered to be very sensitive since the signal is a subtle variation of a large light flux. However, the employment of laser diodes enables measurement of these variations very accurately. For example, an absorption of 10^{-8} causes a change of photon flux which exceeds the fluctuations determined by shot noise if about 5 mW laser power in the red spectral range and a detection bandwidth of 1 Hz is applied. Theoretically, this value corresponds to the detection of about 10 atoms in an absorption path of $L = 10$ cm if the laser beam has a diameter of about 1 mm, a strong resonance line is used, and no optical saturation takes place. In practice, the signal is perturbed by additional noise contributions, such as intensity fluctuations of the laser source (laser noise) and optical interference effects (optical noise). Therefore, various modulation techniques have to be used to transfer the absorption signal into a high frequency range where these noises can be eliminated and measurements at the shot noise limit can be performed. However, it has to be mentioned here that modulation techniques also reduce the absorption signal [11]. In a previous paper, we have investigated and critically analyzed appropriate modulation techniques for diverse noise terms and situations typical for measurements in analytical chemistry [12]. Table 1 recapitulates the noise suppression and detection limits of various modulation techniques (wavelength and absorption modulation) with linear and logarithmic detection, respectively. The signal was linearly processed when only the sample beam was measured. Logarithmic amplification was also employed when the reference beam was measured. The laser wavelength was about 838 nm and the power 2 mW. A detailed discussion of the techniques and their noise suppression is given in reference [12].

Table 1
Noise suppression and detection limits in DLAAS obtained with 2 mW laser power, different modulation techniques, and linear (single beam scheme) and logarithmic (double beam scheme) signal processing

Modulation scheme	Detection	Noise suppression	Detection limit ($[\mathrm{AU}/\sqrt{\mathrm{Hz}}]$)
Wavelength	Linear	Laser excess noise	$\approx 10^{-5}$
Wavelength	$\ln(I_S/I_R)$	Laser excess noise[a]	$\approx 10^{-5}$
Wavelength + absorption	Linear	Laser- and optical-excess noise/RAM noise	$\approx 10^{-6}$
Wavelength + absorption	$\ln(I_S/I_R)$	Laser- and optical-excess noise/RAM noise[a]	$\approx 10^{-7}$

[a] Total suppression of laser excess noise.

In order to determine the detection limit which can be achieved applying a definite modulation $\omega(t) = \omega_0 + m\sin(\omega_{\mathrm{mod}}t)$, we have to calculate the value of the modulated signal corresponding to the extinction of κL (κ is the absorption coefficient). The amplitude of the (modulated) signal is $i(\kappa L/2)$, where i is the current of the photodetector in the absence of absorption.

Based on the relation between the modulation depth m and relevant noise terms, optimum S/N-ratios in WM-DLAAS are generally obtained at second harmonic detection [11], though the peak signal is slightly reduced in comparison with direct absorption and amounts, in the case of a Lorentzian line shape, to about $0.35i(\kappa L/2)$.[2] This means that an absorption of $0.18\kappa L$ can be distinguished with high significance from noise.

Moreover, taking into account the internationally accepted 3σ criterion for detection limits (σ is the standard deviation of the noise $\Delta i_{\mathrm{noise}}$), the smallest detectable absorption is:

$$A_{\mathrm{min}} = \frac{3}{0.18}\frac{\Delta i_{\mathrm{noise}}}{i} \approx 17\frac{\Delta i_{\mathrm{noise}}}{i} \quad (1)$$

for the considered Lorentzian line.

On the other hand, shot noise is described by $\Delta i_{\mathrm{shot}} = \sqrt{2ei\Delta f}$. Therefore, the detectable absorption — given by (1) — is limited to

$$A_{\mathrm{min}} \approx 17\frac{\Delta i_{\mathrm{shot}}}{i} \approx 25\sqrt{\frac{e\Delta f}{i}} \quad (2)$$

where e denotes the charge of the electron and Δf is the detection bandwidth.

[2] About $0.44i(\kappa L/2)$ for a Gaussian line [11].

This means, for example, that a photocurrent of 3 mA corresponds to a smallest detectable absorption of $A_{min} = 1.7 \times 10^{-7}$ within a bandwidth of 1 Hz, which is a typical situation for measurements with laser diodes. Such low absorption measurements have been demonstrated in our laboratory [12]. On the other hand, A_{min} amounts to 2.5×10^{-5} if radiation powers of about 1.5 μW (0.15 μA photocurrent) are applied. The latter absorption limit is typical for the chromium measurements reported in the present paper.

The LDR of DLAAS can be many orders of magnitude. The upper limit corresponds to an absorption of about 1% while the lower limit is given by the detection limit. If the detection limit is of the order of 10^{-7} to 10^{-6} the LDR is four to five orders of magnitude [13].

3. Experimental arrangement for DLAAS in chromatography

DLs have typical powers of several mW and operate in the blue, red and near infrared range of the electromagnetic spectrum. Commercially available DLs produce light at wavelengths of 375–450 nm and >620 nm for the blue and red/NIR, respectively [10,14]. Most useful atomic lines for AAS are in the UV or blue region, and hence frequency doubling of the DL radiation is necessary if the transition wavelengths are outside 375–450 nm. Until quite recently, the only technique to access these wavelengths for DLs involved second harmonic generation (SHG) using a bulk frequency doubling crystal, which is a very inefficient process, producing typical powers of 10–100 nW. The shot noise limit for this power is approximately 10^{-4} absorption units (AU). Recently, quasi phase-matching (QPM) structures for frequency doubling [14–16] became commercially available. These devices, which can be used at wavelengths above 320 nm, are based on periodically poled nonlinear crystals and have a much higher efficiency — up to 1% at 100 mW of DL power. This innovation improves the performance of the DLAAS instrumentation and makes the method applicable for about 40 elements. Table 2 shows the elements that can be excited directly with commercially available DLs (in the red/NIP or blue) or by frequency doubling of DL radiation with QPM structures (in the UV and blue).

In Table 2 we have also listed strong absorption transitions of 40 different metals whose wavelengths can be reached with commercially available laser diodes, either directly applying the fundamental wavelengths or by frequency doubling. The initial states of the absorption transitions are the ground states or states which are highly populated by thermal collisions in the absorption volume. Table 2 could include even more metallic elements if also weaker absorption transitions are included. Non-metallic elements, such as the halogen elements, carbon, sulfur or hydrogen have resonance transitions in the far UV which are far from the wavelengths reached by frequency doubled diode laser radiation. However, most of these elements have strong absorption transitions from their metastable levels in the red and NIR range where commercial laser diodes operate. Relatively high population densities of metastable atoms can be produced in low-pressure plasmas, where the collisional depopulation is low. Table 3 shows those non-metallic elements with their strong absorption lines which can be sensitively detected by DLAAS in low-pressure discharges.

Table 2
Determinable elements (metals) by DLAAS

Element	Wavelength (nm)
Elements accessible by second harmonic generation	
Ag	328.07
Ba	350.12
Co	347.4
Cu	324.7
Eu	333.44
Fe	344.07
Hf	333.2
Lu	331.21
Ni	335.96
Os	325.79
Re	346.05
Rh	343.49
Ru	342.83
Th	330.4
Ti	334.19
Tl	377.57
V	318.39
Zr	341.47
Elements directly accessible with DLs	
Al	396.1
Ca	422.7
Cr	425.4
Cs	852.14
Ga	403.31
Gd	404.5
Ho	405.4
In	410.1
K	766.49
La	407.92
Li	670.78
Mn	403.08
Mo	390.3
Nb	410.09
Nd	454.22
Rb	780.0
Sc	405.45
Sm	380.4
Tb	431.89
Tm	409.42
U	404.27
Y	407.74

The basic experimental arrangement for speciation analysis with DLAAS detection is shown in Fig. 1. The spectral output of a laser diode or of a frequency doubled diode laser system is passed through a continuous atomizer which can be plasma or a simple analytical flame coupled to the chromatograph. The wavelength of the diode laser system is tuned to the absorption transition of interest changing the temperature of the laser diode [10]. Here, at stable temper-

Table 3
Determinable non-metallic elements by DLAAS using electronically excited, metastable state population in a low-pressure plasma

Element	Wavelength (nm)
H	656.28
He	667.82
C	833.74[a]
N	746.83
O	777.75
F	685.79
Ne	640.40
S	921.29
Cl	837.59
Ar	811.75
Br	827.47
Kr	811.56
I	906.08
Xe	823.16
Rn	745.00

[a] Lower level resonant.

ature, the laser wavelength is modulated by variation of the laser diode current to obtain low-noise absorption signals from the photodetector behind the atomizer. Usually, the photodetector is a low-noise silicon photodiode, or, in some cases, a photomultiplier tube.

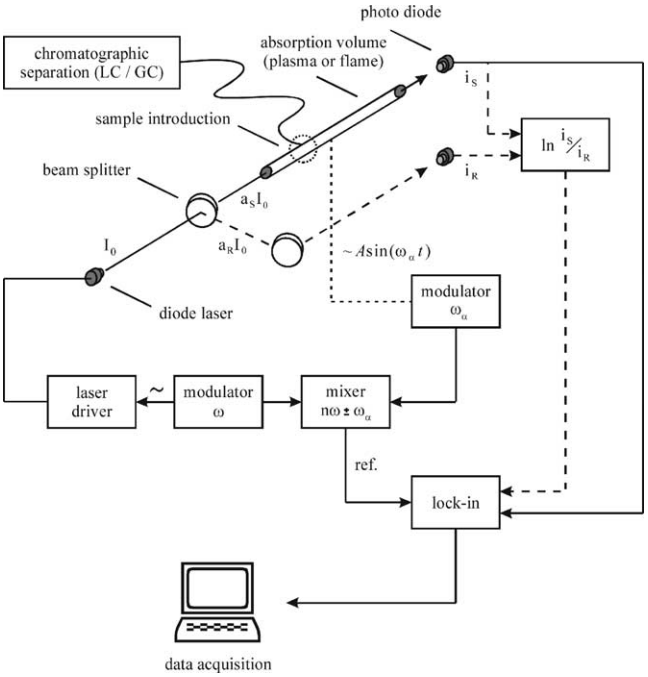

Fig. 1. Experimental arrangement for element-selective detection by DLAAS in chromatography. The laser radiation applied can be the fundamental or the frequency doubled (not shown in the figure) output of a diode laser system and the continuous atomizer of the chromatographic eluates a plasma or a flame. The wavelength of the laser diode has to be modulated across the absorption line and the absorption signal is phase-sensitively detected. Optionally, a reference beam for normalization, modulation of the absorption (in particular for plasma atomizers), and logarithmic processing of the signal can be applied to achieve ultimate sensitivities. This is shown by dashed lines.

If DLAAS measurements with wavelength modulation are not shot noise limited due to low radiation power, as may occur with frequency doubling, it is of advantage to use a double beam arrangement as discussed above and shown in Fig. 1. In some cases, e.g. with plasma atomizers, there is the additional ability to modulate the absorption by switching the plasma on and off. The absorption signal normalized by the reference signal is phase-sensitively detected at the sum or difference frequency of the wavelength and absorption modulation frequencies or its higher harmonics. Almost shot noise limited absorption (2×10^{-7} absorption) at relatively high laser powers (2 mW) has been demonstrated applying logarithmic processing of the absorption signal [12]. Details of the double beam, double modulation technique with logarithmic detection are given, for example, in references [12,17].

4. Experiment and discussion

4.1. Metal speciation analysis

4.1.1. Chromium(III) and chromium(VI)

The determination of chromium(III) and chromium(VI) in the environment is a well-known problem. Chromium(III) is regarded as a nutritionally essential element that is linked to glucose and lipid metabolism in mammals [18]. The estimated safe and adequate dietary intake is 50–200 μg for an adult [19]. Chromium(VI), however, is significantly more toxic than chromium(III), producing liver and kidney damage, respiratory disorders, and internal hemorrhage [19–21]. In addition, inhalation exposure of Cr(VI) has been shown to induce lung cancer. Skin contact may cause allergies and dermal corrosion. The higher toxicity of Cr(VI) has been linked to the ease through which it crosses cell membranes and its high oxidative potential. The US Environmental Protection Agency (EPA) has established Preliminary Remediation Goals (PRGs) of 55 000 μg/L for Cr(III) and 110 μg/L for Cr(VI) in drinking water, illustrating the differences in toxicity between the two oxidation states [21].

Chromium is the 21st most abundant element in the crust of the earth [19,20]. It is employed in a variety of industrial applications, including metallurgical applications (steel production), as pigments for paints and other products, and in wood preservatives. Because of its industrial importance, large quantities of chromium are discharged into the environment. The speciation of this element is further complicated because Cr(III) and Cr(VI) are in dynamic equilibrium. Chromium(III) is favored by low pH, anaerobic conditions, and high amounts of organic matter. In addition, chromium(III) adsorbs onto clay and other negatively charged particles, while Cr(VI) is more water-soluble and mobile. It is clearly desirable to have high sensitivity, low cost instrumentation to distinguish between these two forms of chromium to evaluate toxicological effects and

distribution, transport, and chemical transformations in the environment.

ICP-MS has excellent analytical sensitivity for chromium speciation analysis. However, interferences with polyatomic ions effect Cr(VI) determination at sub-μg/L concentration levels [22]. Moreover, these interferences restrict the chromatographic conditions usable for ICP-MS. For example, our ion-pair chromatography system, which allowed on-line preconcentration of Cr(VI), employed a mobile phase containing 40% of methanol and cannot be coupled with ICP-MS due to a strong interference of $^{40}Ar^{12}C^{+}$ with $^{52}Cr^{+}$ unless a sector field mass spectrometer with sufficient resolution is used. As a result, DLAAS coupled with the ion-pair chromatography provided a significantly better detection limit for Cr(VI) determination than ICP-MS. In addition, DLAAS is more compact and robust, making DLAAS the method of choice for Cr(III)/Cr(VI) speciation analysis.

The capability of DLAAS employing simple analytical flames in combination with HPLC and a high pressure nebulization system for the Cr(III)/Cr(VI) speciation analysis has first been shown in [23]. The power of the frequency doubled radiation was only 70 nW since we used $LiIO_3$ as non-linear medium for 50 mW fundamental radiation from a laser diode. Although the detection limit was already very low (about 1 ng/mL), it was too high to detect Cr(VI) in ordinary drinking water. In more recent work, a SHG power of about 3 μW was generated in a more efficient crystal ($KNbO_3$). The increase of radiation power improved the detection limit significantly and allowed us to detect Cr(VI) in tap water far below the level which is considered as toxic [24].

For quantitative chromium speciation analysis by DLAAS, the atomizer in the basic experimental arrangement (Fig. 1) is a flame and the chromatograph a HPLC system. An AlGaAs-type laser diode (SDL-5410, wavelength at room temperature: 853 nm, maximum output power: 50 mW) driven by a commercial laser diode controller (LDC 400 by Profile) was used. The wavelength of the laser diode was modulated sinusodially using a commercial function generator (Wavetec FG 5000) at a frequency of 7.5 kHz. As already mentioned above, the collimated laser radiation was frequency doubled in a $KNbO_3$ crystal which was temperature tuned for phase matching. The atomizer was a commercial air-acetylene flame (Varian).

The specific Cr absorption ($3d^5 4s^7S_3 \rightarrow 3d^5 4p^7P_3$ transition at 427.48 nm) was measured by a low noise silicon photodiode applying phase sensitive amplification at the second harmonic of the wavelength modulation frequency. Moreover, we applied a double beam detection scheme with logarithmic subtraction similar to the arrangement described in [12] in order to compensate for the background component at the second harmonic of diode laser modulation frequency. This component arises by SHG in the nonlinear crystal, where fluctuations cause additional noise. The 2f signal of the lock-in amplifier (Stanford Research Systems SR-830) was fed into a personal computer via an analog–digital PC board with a sampling rate of 3 Hz.

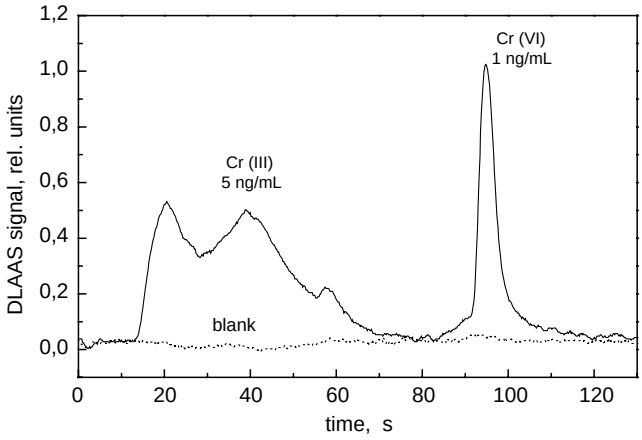

Fig. 2. Cr(III)/Cr(VI) speciation of a spiked water sample by HPLC and DLAAS in a flame.

A commercial HPLC system (Knauer) with a Eurosphere Rp C_{18} chromatographic column (also from Knauer) was used. The chromatographic separation required a special preparation procedure, consisting of the admixture of acetic acid to reach a definite pH value and tetrabutylammonium acetate for the ion-pairing process. Sample volumes of 1 mL were introduced into the HPLC system. A detailed description of the full procedure is given in [25].

Fig. 2 shows a chromatogram for a water sample spiked with 5 ng/mL Cr(III) and 1 ng/mL Cr(VI). While the Cr(VI) peak is relatively narrow, due to on-line preconcentration by the chromatographic procedure, the Cr(III) signal is quite broad due to the presence of various Cr(III) complexes. The high detection power of our instrument was demonstrated by the determination of Cr(VI) in tap water. The Cr(VI) concentration varied from 400 to 50 pg/mL, depending on the day and time of measurement. As expected, higher concentrations were obtained early in the morning. Fig. 3 shows, for example, the signal of a sample taken directly after opening

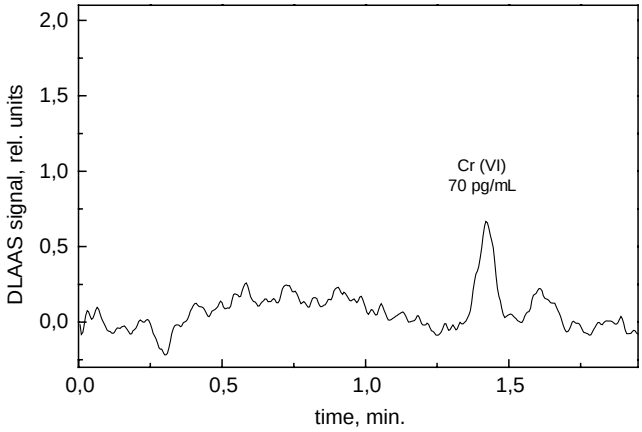

Fig. 3. Chromatogram Cr(VI) in tap water measured by HPLC and DLAAS in a flame.

the tap in the morning and taken after the water was allowed to flow for 10 min. The detection limit was determined to be 30 pg/mL which corresponds to about 1.4×10^{-4} absorption (band width: 0.5 Hz). The experimental detection limit was very near to the theoretical one.

It has to be stressed that similar detection limits in chromium speciation analysis can only be expected if ICP-MS with a sector field mass spectrometer is used in combination with HPLC. However, ICP-MS is a bulky and expensive technique which is certainly much more difficult to use for on-line control than the simple and compact flame-DLAAS technique.

4.1.2. Speciation analysis of organic and inorganic manganese compounds by HPLC-DLAAS

Considerable controversy has developed over the potential toxicity of a fuel additive, methylcyclopentadienyl manganese tricarbonyl [26,27]. From 1977 to 1995, MMT was approved only for limited use in leaded gasoline at a concentration level of 9 mg (as Mn)/L. During this period, the manufacturer made several applications to the US Environmental Protection Agency for permission to market MMT for use in unleaded gasoline. Although these applications were denied, the manufacturer was able to successfully challenge the denial in federal court. Consequently, MMT has been marketed in the United States since December, 1995.

Although manganese is considered a nutrionally essential trace element, it is clear that very high levels of inhaled manganese induce neurobehavioral and respiratory effects [26–29]. The major manganese-containing compounds were manganese sulfate, manganese phosphate, Mn_3O_4, and MnO. The health risks associated with a potential widespread introduction of MMT into the US gasoline supply, which would probably cause relatively small increases in inhaled manganese, remain unknown because of limitations in data. These include limited knowledge of the toxicity of MMT and its combustion products and considerable uncertainty in exposure assessments of MMT.

In addition to the combustion of manganese, human exposure to MMT may also occur through surface water and ground water ecosystems [30]. The addition of MMT to gasoline may increase gastronomical absorption of the compound. Workers at MMT production facilities, refineries, fuel terminals, and service stations may sustain direct exposure to the chemical. In addition, manganese emissions from tailpipes are expected to contaminate soil near roads. This may lead to ingestion of manganese-contaminated soil by children.

The widespread introduction of MMT into the United States gasoline supply has the potential to be a serious threat to public health [27]. It may be necessary to routinely monitor gasoline, ground water, and human fluids (e.g., urine, blood) to evaluate potential human exposure. Toxicological experiments of MMT and its metabolites on animals are required to assess the effects of these compounds on human health, with particular emphasis on “at risk” populations which include MMT production facility workers, service station attendants, children, and pregnant women. The development of high sensitivity, low-cost, reliable instrumentation will allow research and monitoring laboratories to make these important measurements.

One of the deficiencies of most previous studies of MMT is the analysis typically consisted of the measurement of total levels of manganese, rather than speciation of the compounds present. MMT is considerably more toxic than most inorganic forms of manganese. Differences in toxicity exist among inorganic manganese compounds, with manganese(III) more toxic than manganese(II) [16,28,30].

We have applied HPLC-DLAAS instrumentation described above for the determination of inorganic manganese, MMT and its nonmethylated derivative, cyclopentadienyl manganese carbonyl (CMT) [31]. In this study, a near-infrared laser diode was employed to produce laser light at 806.2 nm which was then frequency doubled to produce radiation at 403.1 nm for manganese determination. The detection system included a photomultiplier tube, logarithmic amplifier, and a lock-in amplifier. Data processing was performed with a personal computer. Reversed phase HPLC was employed to separate the manganese-containing compounds. The chromatographic conditions were optimized, and detection limits, linear dynamic ranges, and analysis times were obtained for DLAAS with and without HPLC.

Fig. 4 shows a typical chromatogram of 50 ng/mL of inorganic manganese, 50 ng/mL of CMT, and 50 ng/mL of MMT using 65:35 methanol/pH 4 buffer [31]. Inorganic manganese was not retained and eluted at 0.5 min, CMT eluted at 1.8 min, and MMT eluted at 2.5 min. In the absence of the column, direct DLAAS analysis provided total manganese determination in less than 1 min.

The organomanganese compounds are characterized by rapid decomposition in sunlight (half-life of 0.93 min) [32], and hence we investigated the stability of these compounds in polyethylene bottles under normal laboratory lighting conditions. Fig. 5 shows the decomposition of 50 ng (as

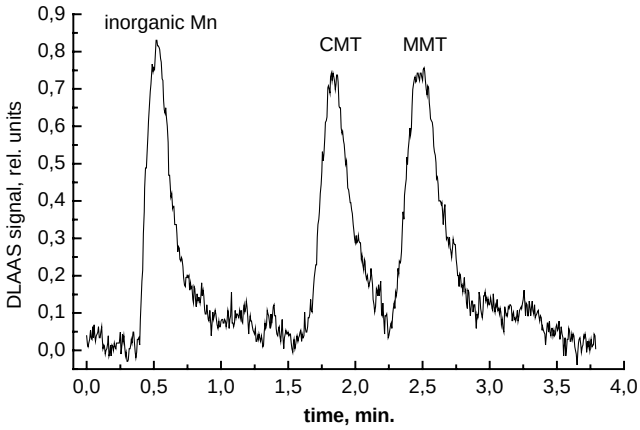

Fig. 4. Chromatogram of inorganic manganese, CMT and MMT (concentrations are 50 ppb each) measured by HPLC and DLAAS in a flame.

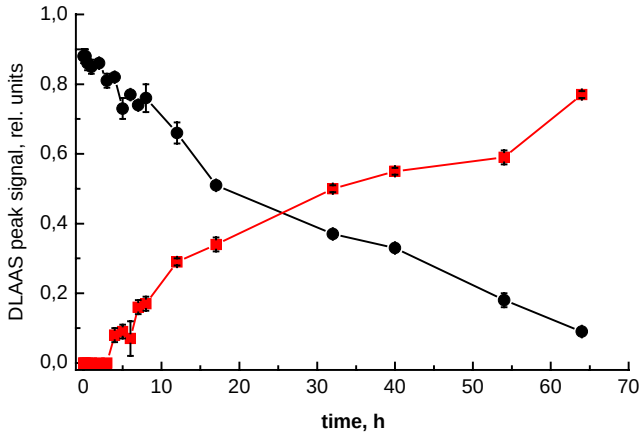

Fig. 5. Decay of the MMT in a polyethylene bottle due to light (●) and increase of the inorganic Mn signal (■).

Mn)/mL MMT over more than 2 days [31]. Minimal degradation was observed over the first 3 h of the experiment. These results indicate that little degradation would occur during normal sample introduction procedures, but that the solutions should be stored in light-tight containers at other times. Significant degradation occurred at longer exposure times in approximately a linear relationship, although complete degradation was not observed after more than 2 days.

Table 4 is a comparison of analytical figures of merit for DLAAS and for other competitive techniques [31]. In terms of detection limit, the DLAAS value of 1 ng/mL was a factor of three better than the best reported hollow cathode lamp atomic absorption spectrometry (HCLAAS) detection limit. This relatively small difference in sensitivity is caused by two factors. First, the DLAAS measurement was made at 403.1 nm, which is 10 times less sensitive than the HCLAAS wavelength at 279.5 nm. Second, our measurement was made at a relatively low laser power, and a significant improvement would be expected by increasing the laser power. Our detection limit was a factor of 3 and 200 worse than standard values for ICP-OES and ICP-MS, respectively. However, even with the limitations of this experimental set-up, we were able to detect manganese compounds at concentration levels necessary for environmental and toxicological studies.

Table 5
Comparison of analytical figures of merit of HPLC-DLAAS to HPLC-LEAFS for determination of inorganic manganese, CMT, and MMT [31]

Figure of merit	HPLC-DLAAS[a] [31]	HPLC-LEAFS[b] [9]
Mn detection limit (ng/mL (pg))	2 (400)	NR[c]
CMT/MMT detection limit (ng (as Mn)/mL (pg as Mn))	2 (400)	0.5 (10)
Linear dynamic range	3	3
Analysis time (min)	3—routine 6—higher resolution	20

[a] HPLC-DLAAS: high performance liquid chromatography-diode laser atomic absorption spectrometry.
[b] HPLC-LEAFS: high performance liquid chromatography-laser excited atomic fluorescence spectrometry.
[c] Not reported.

Table 5 is a comparison of our HPLC-DLAAS speciation data [31] to a previous HPLC-laser excited AFS (LEAFS) MMT speciation study [9]. Our concentration detection limits are within a factor of 4 of the literature values, but the absolute detection limit was 40 times higher. This disparity was caused by our use of a larger injection loop (0.2 mL compared to 0.02 mL). The linear dynamic range for both systems was three orders of magnitude. One advantage of our chromatographic conditions was the speed of the analysis (3 min), with good resolution using 65:35 methanol/aqueous pH 4 buffer as the mobile phase. Higher resolution was obtained using a mobile phase of 60:40 methanol/aqueous pH 4 buffer, although the analysis time was increased to 6 min.

MMT was added to samples of gasoline, human urine, and tap water, and determined by HPLC-DLAAS [31], and the results are summarized in Table 6. These samples were selected because of their environmental and toxicological significance. The spiked samples were diluted to give MMT concentration levels between 40 and 100 ng/mL for analysis. Aqueous calibration graphs were constructed to quantify the samples. The sample matrices did not effect the retention time and peak shapes of the analyte, probably because our low detection limits allowed large dilution factors to be employed. In all cases, good agreement was obtained between the expected concentration and the concentration determined by HPLC-DLAAS. In summary, HPLC-DLAAS

Table 4
Comparison of analytical figures of merit of DLAAS to other techniques for determination of inorganic manganese, CMT, and MMT [31]

Figure of merit	DLAAS[a] [31]	HCLAAS[b] [5]	ICP-OES[c] [7]	ICP-MS[d] [8]
Mn detection limit (ng/mL)	1	3	0.3	0.0005
CMT/MMT detection limit (ng(as Mn)/mL)	1	NR[e]	NR[e]	NR[e]
Linear dynamic range (orders of magnitude)	4.7	3	5	8

[a] DLAAS: diode laser atomic absorption spectrometry.
[b] HCLAAS: hollow cathode lamp atomic absorption spectrometry.
[c] ICP-OES: inductively coupled plasma-optical emission spectrometry.
[d] ICP-MS: inductively coupled plasma-mass spectrometry.
[e] NR: not reported.

Table 6
Analysis of samples spiked with MMT [31]

Sample	Added concentration (μg (as Mn)/mL)	Reported solubility in water (μg (as Mn)/mL) [30]	Determined value by HPLC-DLAAS (μg (as Mn)/mL)
Gasoline	8.3	–	8.0 ± 0.8
Human urine	4.0	–	4.2 ± 0.3
Tap water	–	10, 29, 70	36 ± 2

was shown to be a sensitive, selective, rapid, and accurate technique for MMT determination.

4.2. Element-selective detection of non-metals in GC

The element-selective DLAAS detector in GC requires a plasma which replaces the more general atomizer in Fig. 1. It can be a plasma at ambient pressure for the determination of metallic elements. However, it has to be operated at reduced pressure for non-metals.

The gas chromatograph we have in our laboratory is a Shimadzu GC-14A with a fused silica column FS-SE-54-CB-1 (column-length: 50 m; inner diameter of column: 0.32 mm) with helium as carrier gas. The outlet gas flow of the column is directed through a quartz capillary (diameter 2 mm) where a microwave-induced plasma (MIP) is sustained. The MIP operates in a Beennaker-type resonator [33] at a pressure of about 20 mbar. The radiation of the laser diode is directed through the plasma on a silicon photodiode. For example, the laser diode is tuned to the chlorine $3p4s^4P_{5/2} \rightarrow 3p4p^4D_{7/2}$ absorption line at 837.60 nm (see Table 3) which probes the density of metastable Cl atoms in the plasma. The wavelength of the laser diode is typically modulated with a frequency of $f_{laser} = 11.5$ kHz. Additionally, the plasma can be modulated with a frequency of $f_{plasma} = 5$ kHz. The signal is detected at the mixed frequency $f = 2f_{laser} - f_{plasma} = 18$ kHz. This double modulation arrangement improves the S/N-ratio significantly as mentioned above [12,13].

Typical carbon-, chlorine- and hydrogen-specific chromatograms of eight different species are shown in Fig. 6. Evaluating the chromatograms one finds that the ratios of the absorption signals represented the stoichometry of the elements in the species. This a pre-condition for the application of internal standards. In reference [34], we used $C_5H_{11}Cl$ to determine the concentrations of the other species C_7H_{16}, C_6H_5Cl, C_8H_{14}, C_8H_{16}, and $C_4H_8Cl_2$. There was only a slight deviation for the carbon-specific stoichiometry for chlorobezene (C_6H_5Cl). The reason for this deviation could not be found.

Chlorine-, carbon- and hydrogen-specific calibration graphs were made in order to determine the analytical detection limits of the DLAAS arrangement with respect to gas chromatographic eluents. Therefore, the analyte concentration of a matrix, consisting of $C_5H_{11}Cl$, $C_3H_6Cl_2$, and C_6H_5Cl was successively reduced and subsequently quantified. In contrast to the stoichiometric measurements, the separated compounds were sequentially analyzed. For example, the chlorine- and hydrogen-specific detection limits of $C_5H_{11}Cl$ were of the order of 60 and 300 pg, respectively, while the carbon-specific calibration resulted in an average detection limit of about 5 ng. This high value is a consequence of the weak population density of the resonant C $3s^1P_1^0$ initial state as well as the moderate oscillator strength of the used $3s^1P_1^0 \rightarrow 3p^1S_0$ transition.

4.2.1. Measurement of volatile chlorinated hydrocarbons in oil

The analytical problem in this example was the determination of low concentrations of volatile chlorinated hydrocarbons in the oil samples of an industrial plastic material recycling process. These analytes could not be measured by a commercial AES detector because of its insufficient sensitivity [35]. These species were of interest in an industrial process since they poisoned the catalysts and attacked the reactor wall at very low concentrations. The samples were measured with our experimental GC arrangement employing

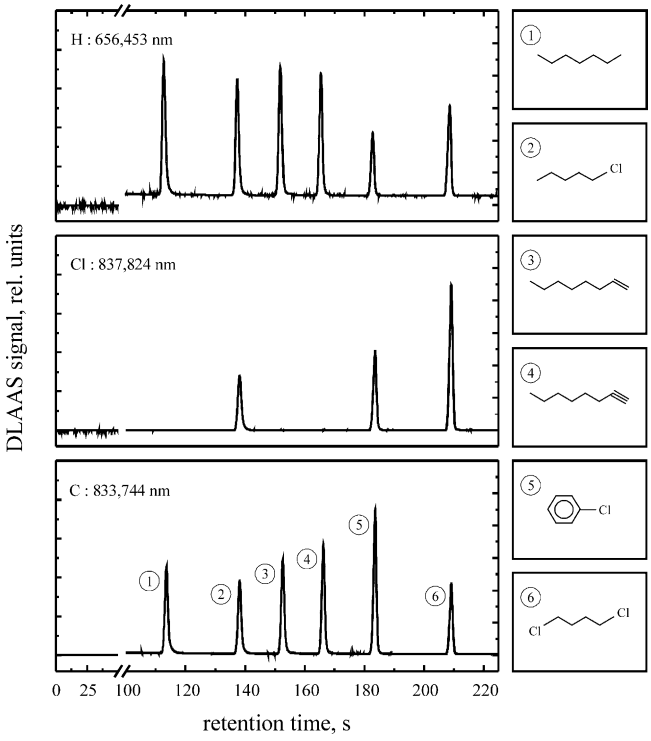

Fig. 6. Chromatograms of a sample with 1.2 mg/mL of heptane (1), 1-chloropentane (2), 1-octene (3), 1-octyne (4), chlorobenzene (5), and 1,4-dichlorobutane (6) each measured by GC and DLAAS of H, Cl and C in a low-pressure He plasma.

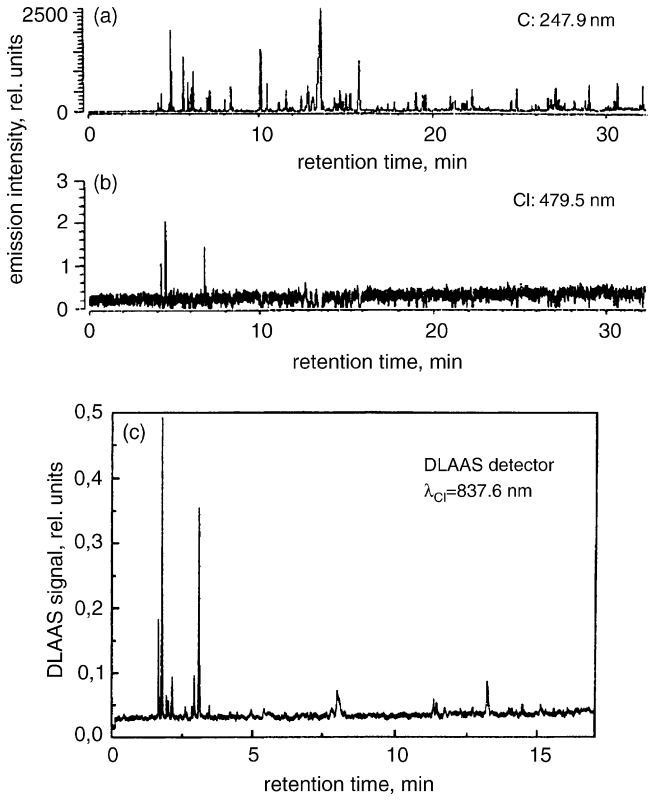

Fig. 7. GC chromatograms of an oil sample from a plastic recycling process measured by element-selective detection applying a commercial AES detector ((a) C 247.9 nm line, (b) Cl 479.5 nm line) and the DLAAS detector.

a low-pressure MIP which was also used in the stoichiometry experiment reported in the preceding chapter. Fig. 7 shows a comparison of chromatograms obtained with the DLAAS (Fig. 7c) and a commercial AES detector (Fig. 7a and b) analyzing an oil sample with elevated concentration of volatile chlorinated hydrocarbons. While the DLAAS chromatogram was measured using the 837.60 nm Cl absorption line, Cl and C were determined by the AES detector using the 479.45 and 247.86 nm emission lines, respectively. The experimental conditions were as follows: injection of a 0.5 μL sample, a split ratio of 1:20, and dilution of the eluate in the low-pressure MIP by a ratio of 1:3. A more detailed description of the experimental conditions can be found in the original paper [35]. The concentrations of the chlorinated hydrocarbons at the beginning of the chromatograms of Fig. 7 were found to be of the order of 5–20 μg/mL. A DLAAS detection limit of about 100 ng/mL was obtained for the chlorinated species which is comparable with the detection limits obtained for undiluted haloform standard samples [13].

4.2.2. Measurement of chlorophenols in plant extracts

Chlorine-selective chromatograms of a standard sample and of a plant extract in *n*-hexane are shown in Fig. 8. While the standard sample contained different types of chlorophe-

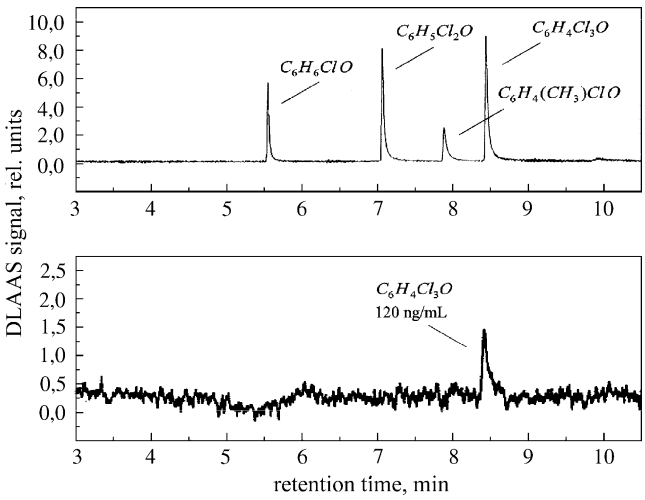

Fig. 8. Cl-selective chromatograms of a chlorophenol standard (top) and an extract from a plant exposed to TCP (bottom). The DLAAS detector was tuned to the Cl 837.6 nm line, the continuous atomizer was a low-pressure plasma.

nols, only trichlorophenol (TCP: $C_6H_4Cl_3O$) was detected in the plant sample. The plant had been previously exposed to TCP in a greenhouse. TCP was extracted from the wax layer of leaves or needles by dichloromentane with 0.1 M potassium carbonate added. Sample volumes of 1 μL were injected into the gas chromatograph. A detection limit of 30 ng/mL for TCP was obtained [35].

The advantage of element selective detection by DLAAS can be seen if Fig. 8 is compared with Fig. 9, which

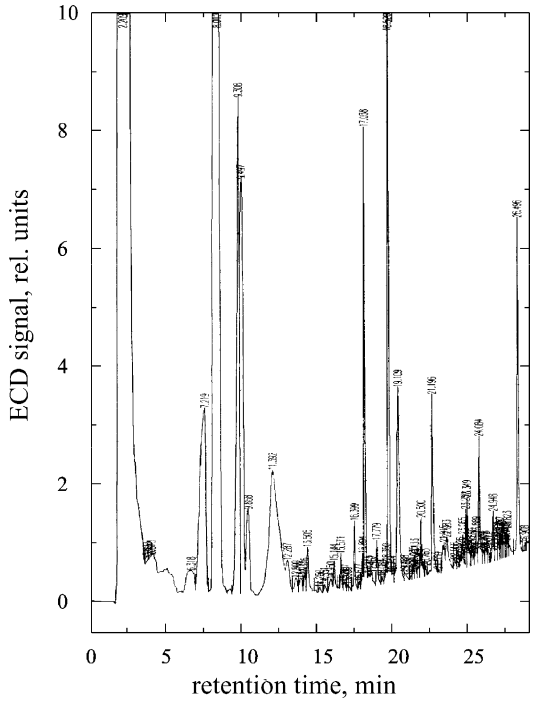

Fig. 9. Non-selective chromatogram of the TPC exposed plant sample of Fig. 8 measured with a commercial ECD-detector.

displays a chromatogram of the plant measured with the non-element specific electron capture detector (ECD). The ECD, which exhibits different sensitivities for different molecular species, is commonly used for chlorophenol measurements. The ECD chromatogram of the plant extract shows many components which do not contain Cl atoms and hence the TCP signal could hardly be seen. Furthermore, it has a sloping background because of overlapping components. Therefore, it is very hard to discriminate a small TCP signal from other components and, if one has located the chlorophenol, to give the exact magnitude of the signal. In comparison, the DLAAS-detector chromatogram shows only Cl containing components, and in our case, only the TCP signal. Furthermore, there is the possibility of calibration by the addition of internal standards containing Cl or other elements because the element-selective signals reflect the stoichiometric ratios of the elements in the species [13,34]. Element selective detection in GC has been demonstrated not only for Cl but also for F and Br [13], and I and S [36].

It is not surprising that the results of an inter-laboratory comparison studies of the TCP-containing plant samples was not very successful since ECD's were applied in all other measurements. The TCP concentration found by different laboratories with ECD varied about three orders of magnitude because of the strong interferences of the TCP signal with other matrix components. AED's were not employed because the detection limits were not sufficiently low.

5. Conclusion

In conclusion, DLAAS is a sensitive, low cost, robust, and compact technique for element-selective detection in speciation analysis. It offers low detection limits and a large dynamic range, in special cases about four orders of magnitude. The restricted wavelength ranges of laser diodes have limited the number of elements to which this technique has been applied. Frequency doubling of diode laser radiation improves the situation, however, at the expense of detection limits. We anticipate DLAAS has a bright future for element-selective detection in chromatography once diode lasers cover a larger spectral range and have higher output powers to permit more efficient frequency doubling.

References

[1] R.M. Harrison, S. Rapsomanikis (Eds.), Environmental Analysis using Chromatography Interfaced with Atomic Spectroscopy, Halsted Press, New York, 1989.
[2] S. Caroli (Ed.), Element Speciation in Bioinorganic Chemistry, Wiley, New York, 1996.
[3] S.J. Hill, S. Chenery, J.B. Dason, E.H. Evans, A. Fisher, W.J. Price, C.M.M. Smith, K.L. Sutton, J.F. Tyson, J. Anal. Atom. Spectrom. 15 (2000) 763.
[4] L. Ebdon, S. Hill, R.W. Ward, Analyst 112 (1987) 1.
[5] B. Welz, Atomic Absorption Spectrometry, third ed., Wiley, New York, 1998.
[6] D.J. Butcher, J.A. Sneddon, Practical Guide to Graphite Furnace Atomic Absorption Spectrometry, Wiley, New York, 1998.
[7] A. Montaser, D.W. Golightly (Eds.), Inductively Coupled Plasmas in Analytical Atomic Spectrometry, VCH, New York, 1992.
[8] A. Montaser (Ed.), Inductively Coupled Plasma Mass Spectrometry, Wiley–VCH, New York, 1998.
[9] A.P. Walton, G.-T. Wei, Z. Liang, R.G. Michel, J.B. Morris, Anal. Chem. 63 (1991) 232.
[10] K. Niemax, A. Zybin, C. Schnürer-Patschan, H. Groll, Anal. Chem. 68 (1996) 351A.
[11] J.A. Silver, Appl. Opt. 31 (1993) 707.
[12] V. Liger, A. Zybin, Y. Kuritsyn, K. Niemax, Spectrochim. Acta Part B 52 (1997) 1125.
[13] A. Zybin, C. Schnürer-Patschan, K. Niemax, J. Anal. Atom. Spectrom. 10 (1995) 563.
[14] K. Niemax, A. Zybin, D. Eger, Anal. Chem. 73 (2001) 134A.
[15] J.A. Armstrong, N. Blombergen, J. Ducuing, P.S. Persham, Phys. Rev. 127 (1962) 1918.
[16] J.P. Meyn, M.M. Fejer, Opt. Lett. 22 (1997) 1214.
[17] J. Koch, A. Zybin, K. Niemax, Spectrochim. Acta Part B 57 (2002) 1547.
[18] J. Kotas, Z. Stasicka, Environ. Poll. 107 (2000) 263.
[19] Ecological Soil Screening Level Guidance, US EPA, Washington, 2000, http://www.epa.gov/oerrpage/superfund/programs/risk/ecorisk/guidance.pdf.
[20] Toxicological Review of Hexavalent Chromium, Washington, 1998, http://www.epa.gov/ngispgm3/iris/toxreviews/cr6-toxf.pdf.
[21] Region 9 Preliminary Remediation Goals (PRGs) 1999, US Environmental Protection Agency, San Francisco, 1999, http://www.epa.gov/region09/waste/sfund/prg.
[22] C. Barnowski, N. Jakubowski, D. Stüwer, J.A.C.J. Broekaert, Anal. At. Spectrom. 12 (1997) 1155.
[23] H. Groll, G. Schaldach, H. Berndt, K. Niemax, Spectrochim. Acta Part B 50 (1995) 1293.
[24] A. Zybin, G. Schaldach, H. Berndt, K. Niemax, Anal. Chem. 70 (1998) 5093.
[25] H. Berndt, A. Müller, Fresenius J. Anal. Chem. 345 (1993) 18.
[26] J.M. Davis, Environ. Health Perspect. 106 (Suppl. 1) (1998) 191.
[27] H. Frumkin, G. Solomon, Am. J. Ind. Med. 31 (1997) 107.
[28] T. Ressler, J. Wong, J. Roos, J. Synchrotron Rad. 6 (1999) 656.
[29] J. Zayed, B. Hong, G. L'Espérance, Environ. Sci. Technol. 33 (1999) 3341.
[30] A.W. Garrison, M.G. Cippolone, N.L. Wolfe, R.R. Swank, Environ. Toxicol. Chem. 14 (1995) 1859.
[31] D.J. Butcher, A. Zybin, M. Bolshov, K. Niemax, Anal. Chem. 71 (1999) 5379.
[32] L. Campanella, Problems in the speciation of elements in natural waters: the case of chromium and selenium, in: S. Caroli (Ed.), Element Speciation in Bioinorganic Chemistry, Wiley, New York, 1996.
[33] C.I.M. Beenakker, Spectrochim. Acta Part B 32 (1977) 173.
[34] J. Koch, K. Niemax, Spectrochim. Acta Part B 53 (1998) 71.
[35] A. Zybin, K. Niemax, Anal. Chem. 69 (1997) 755.
[36] K. Kunze, M. Miclea, J. Franzke, K. Niemax, Spectrochim. Acta Part B 58 (2003) 1435.